Theoretical analysis of the Mackay icosahedral cluster Pd55(PiPr3)12(μ3-CO)20 An open-shell 20-electron superatom

Jean-Yves Saillard, Jianyu Wei, Rémi Marchal, Didier Astruc, Jean-François Halet, Samia Kahlal

10.1002/chem.202000447

WILEY-VCH

FULL PAPER

Theoretical analysis of the Mackay icosahedral cluster $Pd_{55}(P^iPr_3)_{12}(\mu_3\text{-}CO)_{20}$: An open-shell 20-electron superatom*

Jianyu Wei,[a] Rémi Marchal, [a] Didier Astruc, [b] Jean-Yves Saillard,* [a] Jean-François Halet*[a] and Samia Kahlal*[a]

*Dedicated to Professor D. Mike P. Mingos on the occasion of his 75th birthday.

Abstract: The electronic structure of the spherical Mackay icosahedral nanosized cluster $Pd_{55}(P^iPr_3)_{12}(\mu_3\text{-}CO)_{20}$ is analyzed using DFT calculations. Results reveal that it can be considered as a regular *superatom* with a "magic" electron count of 20, characterized by a $1S^2$ $1P^6$ $1D^{10}$ $2S^2$ *jellium* configuration. Its open shell nature is associated with partial occupation of non-*jellium*, *4d*-type, levels located on the interior of the Pd_{55} kernel. This shows that the *superatom* model can be used to rationalise the bonding and stability of spherical ligated group-10, clusters, despite their apparent 0-electron count.

Introduction

In 2016, the first isolation of the crystalline icosahedral Mackay $Pd_{55}(P^iPr_3)_{12}(\mu_3\text{-}CO)_{20}$ (**1**) cluster was reported.[1] This fascinating compound that ideally conforms to I_h symmetry (without isopropyl substituents) is somewhat unique. The Matryoshka doll-like 55-metal-atom two-shell cluster architecture consists of a centered Pd_{13} icosahedron encapsulated within a Pd_{42} icosahedron. In I_h symmetry, the outer icosahedron is made of two different types of symmetry equivalent vertices, of 12 and 30 degeneracy respectively. The whole $Pd@Pd_{12}@Pd_{42}$ metal kernel corresponds to a so-called MacKay "hard-sphere" model.[2] Mackay icosahedra are densely packed assemblies of equal-sized spheres which are characterized by specific numbers of spheres (atoms), 13, 55, 147, 309, etc. forming concentric shells, 1, 2, 3, 4, etc., respectively.[2] The Pd_{55} kernel of **1** is the first crystallographically documented molecular example of a Mackay icosahedron.[1] The 12 outer Pd atoms that are located on the C_5 axis are coordinated by a phosphine ligand, whereas 20 symmetry-equivalent triangular faces of the Pd_{42} outer shell (metal atoms not attached to the 12 phosphine ligands) are capped by carbonyl ligands. The icosahedral two-shell Pd architecture of $Pd_{55}(P^iPr_3)_{12}(\mu_3\text{-}CO)_{20}$ is shown in Figure 1.

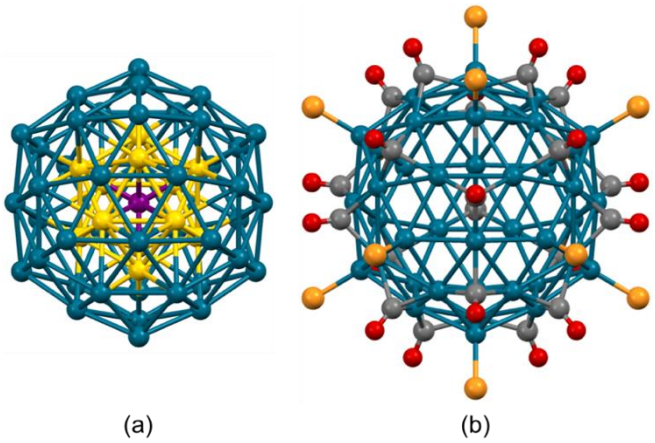

Figure 1. Structural arrangement of $Pd_{55}(P^iPr_3)_{12}(\mu_3\text{-}CO)_{20}$: a) "Matryoshka doll sequence" of the $Pd@Pd_{12}@Pd_{42}$ metal kernel, and b) outer Pd_{42} shell with surrounding ligands (isopropyl groups not shown for clarity). The purple, yellow, dark blue, orange, grey, and red spheres are central Pd (Pd'), inner Pd (Pd"), outer Pd (Pd"'), P, C, and O atoms, respectively.[1]

The structure and bonding properties of stable (viable[3]) inorganic clusters, are usually governed by their numbers of valence electrons. Indeed, as for any stable molecular compound, there are strong relationships between the structure and the electron count of clusters. Such relationships are based on the closed-shell principle and assume that no antibonding orbital is occupied. In the case of organometallic transition-metal clusters, these relationships are issued from the polyhedral skeletal electron pair (PSEP) theory,[4] of which the Wade-Mingos electron-counting rules[5-9] are the most popularized. These rules generally apply well to hollow clusters made of metal atoms, the valence *d* orbitals of which participate to the bonding. This is not the case for group 11 metal clusters, for example, which have their (localized) valence *d* shell filled and then can be ignored in the count of bonding electrons.[10] Thus, group 11 metals participate to the bonding mainly with their valence *s* orbitals. They usually tend to aggregate in a compact (non-hollow) and often spherical way. To understand their structure and composition, the concept of *superatom*,[8-24] based on the spherical *jellium* model, [25-27] is used. This qualitative model considers electrons within a radial phenomenological potential supposed to describe the average electrostatic potential associated with the cluster atom nuclei.

[a] Jianyu Wei, Dr. Rémi Marchal, Prof. Jean-Yves Saillard, Prof. Jean-François Halet and Dr. Samia Kahlal
Univ Rennes, CNRS, Institut des Sciences Chimiques de Rennes (ISCR) – UMR 6226, F-35000 Rennes, France.
E-mail: saillard@univ-rennes1.fr, halet@univ-rennes1.fr, samia.kahlal@univ-rennes1.fr
[b] Prof. Didier Astruc
ISM, UMR CNRS 5255, University of Bordeaux, 351 Cours de la Libération, F-33405 Talence Cedex, France

Supporting information for this article is given via a link at the end of the document.

Thus, the spherical jellium model does not consider explicitly the atom nuclei. On the other side, it allows describing the cluster electronic structure in terms of *superatomic* orbitals, somewhat similar to atomic orbitals, but extending over the whole cluster sphere. Their shell ordering is largely independent from the cluster composition and spans as 1S < 1P < 1D < 2S < 1F, etc. As for atomic systems, closed-shell (noble gas) stability will be achieved for specific ("magic") electron counts, i.e., 2, 8, 18, 20, 34, etc. It is of note that the *superatom* approach considers only the delocalized electrons that are responsible for the bonding within the cluster kernel. In a regular LCAO-MO DFT calculations on group 11 clusters, these electrons are identified as those occupying the Kohn-Sham orbitals of dominant valence *s* character.[10,14-18,20] It turns out that most of the coinage metal clusters isolated so far obey the above-mentioned closed-shell *superatomic* rule.[14-19] It is also noteworthy that in the case of group 11 clusters, both the whole cluster and its metal *superatomic* kernel possess a HOMO-LUMO gap for the considered "magic" electron count. Thus, the external "passivating" shell (the ligands and possibly additional outer metal atoms, all in their actual oxidation states) does not participate to the *superatom* (*jellium*) electron count.

Group-10 clusters of a certain size also tend to aggregate in a compact fashion.[28-32] However, no general electron-counting rules developed for high nuclearity spherical clusters[4] seem to apply to these species in a comprehensive manner. On one side, they often do not obey the classical Wade-Mingos rules. On the other side, the metal oxidation state being generally zero (or close to zero), their *superatomic* electron number is, at least at first sight, also zero (no valence *s* electrons). Dahl's unique atom-precise $Pd_{55}(P^iPr_3)_{12}(\mu_3\text{-}CO)_{20}$ with a total of 614 valence electrons and zero 5*s* electron (assuming Pd(0) $4d^{10}$ $5s^0$ configuration) is a typical example. Several questions arise from its structure and composition: (i) Are both the whole cluster and its isolated Pd_{55} kernel closed-shell entities? (ii) Is the number of 2-electron ligands, i.e., 32, imposed by electronic stability or can it be varied without substantial stability and structural change? (iii) To what extent are the 4*d* and 5*s* metallic orbitals involved in the Pd-Pd and Pd-ligand bonding? And finally, (iv) is the electronic structure of $Pd_{55}(P^iPr_3)_{12}(\mu_3\text{-}CO)_{20}$ somewhat related to that of group-11 *superatoms*? Density functional theory (DFT) calculations were carried out on the title compound, aiming at providing some answers to these questions. The main results are discussed here.

Computational details

Density functional theory (DFT) calculations[33] were performed using the Amsterdam Density Functional (ADF2016) code.[34] Scalar relativistic effects were taken into account via the Zeroth Order Regular Approximation (ZORA).[35] The Vosko-Wilke-Nusair functional (VWN) [36] for the Local Density Approximation (LDA) and gradient corrections for exchange and correlation of Becke and Perdew (BP86 functional),[37,38] together with Grimme's empirical DFT-D3 corrections,[39] were used for geometry optimization and analytical vibrational frequency computation. A triple-zeta basis set, augmented with a polarization function (STO-TZP)[40] for palladium was used. Similar results were obtained with other functionals (see SI). Natural atomic orbital (NAO) populations and Wiberg bond indices (WBIs) were computed using ADF optimized geometries with the natural bond orbital (NBO) 6.0 program,[41] implemented in the Gaussain16 package,[42] at the BP86/Def2-SVP[43] level.

Results and discussion

Three different $Pd_{55}L_{12}(\mu_3\text{-}CO)_{20}$ model clusters were considered in the calculations. The P^iPr_3 ligands of Dahl's compound were first modelized by simple PH_3 phosphines to reduce computational efforts. However, because of the mismatch of the phosphine three-fold symmetry with the five-fold icosahedral symmetry axes, the exact symmetry of the computed cluster was reduced to C_{2h}. Linear L = CO and CNH – the latter possesses electronic properties similar to those of phosphines and allows a higher symmetry of the molecule – ligands were also considered, for which the highest possible cluster symmetry is I_h. The three computed models provided similar results in terms of both their electronic structures and geometries overall. In the following, the L = CO case is analyzed in more details. Since the ADF program does not work with the I_h symmetry group, models with L = CO and CNH were treated in D_{5d} symmetry although the optimized structures were found to be very close to I_h. This is why they are most often described below assuming ideal I_h symmetry.

Table 1. Relevant atomic distances computed for the three optimized neutral models $Pd_{55}L_{12}(\mu_3\text{-}CO)_{20}$ (L = PH_3, CO, CNH) in their triplet ground state configuration. The metal atom labelling corresponds to $Pd'@Pd''_{12}@Pd'''_{42}$. X-ray experimental distances of $Pd_{55}(P^iPr_3)_{12}(\mu_3\text{-}CO)_{20}$ are given for comparison.[1]

$[Pd_{55}L_{12}(\mu_3\text{-}CO)_{20}]$ (L = PH_3, CO, CNH)					
L		PH_3	CO	CNH	Exp.[1]
Average Distances (Å)	Pd'-Pd''	2.636	2.649	2.645	2.63
	Pd''-Pd''	2.772	2.785	2.782	2.76
	Pd''-Pd'''	2.800	2.802	2.800	2.77
	Pd'''-Pd'''	2.845	2.857	2.853	2.83
	Pd'''-L	2.229	1.907	1.918	2.24
	Pd'''-CO	2.092	2.096	2.092	2.07

The three $Pd_{55}L_{12}(\mu_3\text{-}CO)_{20}$ (L = PH_3, CO, CNH) models were found to have a triplet ground state. (Table 1). The lowest singlet states were found to lie 0.83, 0.45 and 0.13 eV above the triplet for L = Ph_3, CO and CNH, respectively. The ground state optimized geometrical data are in a good agreement with the X-ray data of $Pd_{55}(P^iPr_3)_{12}(\mu_3\text{-}CO)_{20}$.[1] A careful analysis of the Kohn-Sham frontier orbitals suggests that a closed-shell ground state configuration should be achieved with two additional electrons accompanied with minor structural differences with respect to their neutral states, *i.e.*, pseudo-I_h symmetry.

10.1002/chem.202000447

FULL PAPER

Table 2. Relevant data computed for the three optimized dianionic models $[Pd_{55}L_{12}(\mu_3\text{-}CO)_{20}]^{2-}$ (L = PH_3, CO, CNH) in their ground state (singlet) configuration. The metal atom labeling corresponds to Pd'@Pd''_{12}@Pd'''. The two different symmetry types of Pd''' atoms are labeled Pd_a''' and Pd_b'''.

$[Pd_{55}L_{12}(\mu_3\text{-}CO)_{20}]^{2-}$ (L = PH_3, CO, CNH)				
L		PH_3	CO	CNH
HOMO-LUMO gap (eV)		0.54	0.58	0.62
Average Distances (Å) [Wiberg indices]	Pd'-Pd''	2.644 [0.078]	2.658 [0.075]	2.655 [0.074]
	Pd''-Pd''	2.781 [0.092]	2.795 [0.092]	2.792 [0.092]
	Pd''-Pd'''	2.798 [0.115]	2.799 [0.112]	2.798 [0.111]
	Pd'''-Pd'''	2.846 [0.069]	2.858 [0.065]	2.855 [0.067]
	Pd'''-L	2.222 [0.475]	1.898 [0.796]	1.902 [0.766]
	Pd'''-CO	2.089 [0.405]	2.092 [0.398]	2.091 [0.402]
Average NAO populations and atomic charges	1 x Pd'	$4d^{9.33}\ 5s^{0.92}\ 5p^{0.04}$	$4d^{9.35}\ 5s^{0.95}\ 5p^{0.05}$	$4d^{9.35}\ 5s^{0.95}\ 5p^{0.05}$
		-0.31	-0.37	-0.37
	12 x Pd''	$4d^{9.48}\ 5s^{0.63}\ 5p^{0.03}$	$4d^{9.48}\ 5s^{0.65}\ 5p^{0.03}$	$4d^{9.49}\ 5s^{0.65}\ 5p^{0.03}$
		-0.17	-0.20	-0.20
	30 x Pd_a'''	$4d^{9.32}\ 5s^{0.45}\ 5p^{0.01}$	$4d^{9.32}\ 5s^{0.45}\ 5p^{0.01}$	$4d^{9.32}\ 5s^{0.45}\ 5p^{0.01}$
		+0.21	+0.21	+0.22
	12 x Pd_b'''	$4d^{9.46}\ 5s^{0.65}\ 5p^{0.02}$	$4d^{9.29}\ 5s^{0.69}\ 5p^{0.02}$	$4d^{9.27}\ 5s^{0.68}\ 5p^{0.02}$
		-0.15	-0.01	+0.02
	42 x Pd''' (av.)	+0.11	+0.15	+0.16
	L	+0.20	+0.01	+0.02
	CO	-0.33	-0.28	-0.31

Calculations on the $[Pd_{55}L_{12}(\mu_3\text{-}CO)_{20}]^{2-}$ dianionic species confirmed this hypothesis, with significant HOMO-LUMO energy gaps of the order of 0.5-0.6 eV (Table 2). As expected, the addition of two electrons hardly affects the interatomic distances of the cluster. The computed Pd-Pd Wiberg indices reflect the interatomic distances and are indicative of moderate metal-metal bonding interactions (Table 2). A glance at the computed natural atomic orbital (NAO) charges reveals some electron transfer from the Pd_{42} *outer* metal shell to the ligand envelope via dπ(Pd)−π*(CO) back-bonding, as well as to the *inner* Pd_{12} shell and central Pd atom (Table 2).[1]

We discuss below the electronic structure of the $[Pd_{55}(CO_{12})(\mu_3\text{-}CO)_{20}]^{2-}$ dianion in more details, before returning to that of the neutral clusters. Its density of states (DOS), plotted in Figure 2, is consistent with a unique favoured closed-shell electron count of 616, corresponding to a dianionic species (similar DOS are computed for $[Pd_{55}(PH_3)_{12}(\mu_3\text{-}CO)_{20}]^{2-}$ and $[Pd_{55}(CNH)_{12}(\mu_3\text{-}CO)_{20}]^{2-}$, see Figure S1 and S2†). A Kohn-Sham diagram of the frontier orbitals of $[Pd_{55}(CO_{12})(\mu_3\text{-}CO)_{20}]^{2-}$ is also provided in Figure 3. Unsurprisingly, the highest occupied states

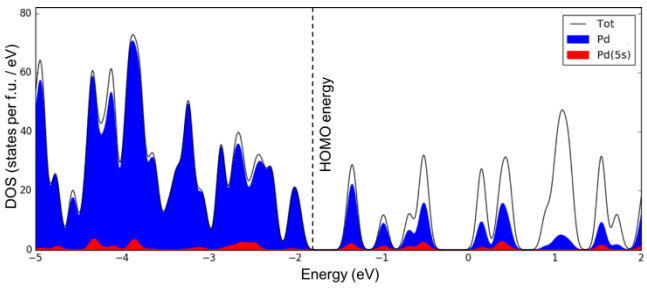

Figure 2. Total, Pd, and Pd(5s) projected DOS of $[Pd_{55}(CO)_{12}(\mu_3\text{-}CO)_{20}]^{2-}$ (Gaussian full width at half maximum (0.1 eV). The dotted line corresponds to the energy of the HOMO.

are of dominant *4d* metal character, while the lowest unoccupied ones have also some π*(CO) admixture.

A detailed analysis of the occupied orbital compositions reveals that ten of them are also of major *5s* (Pd) character. These orbitals are plotted in Figure 4. They can be easily identified as the 1S, 1P, 1D and 2S *superatomic* ("*jellium*") orbitals. The lowest

10.1002/chem.202000447

one (1S) is strongly bonding and lies below the whole block of the *4d* states. The highest one (2S) is still significantly bonding and situated 0.79 eV below the HOMO. Thus, with a $1S^2\ 1P^6\ 1D^{10}2S^2$ configuration, $[Pd_{55}(CO_{12})(\mu_3\text{-}CO)_{20}]^{2-}$ is a 20-electron *superatom*. Assuming that Pd(0) is $4d^{10}5s^0$, one should expect only one of the *5s* combinations occupied by the two electrons associated with the -2 charge. Since ten *5s* combinations are actually occupied in the dianionic clusters, it means that nine *4d*-type combinations have formally transferred their electrons to

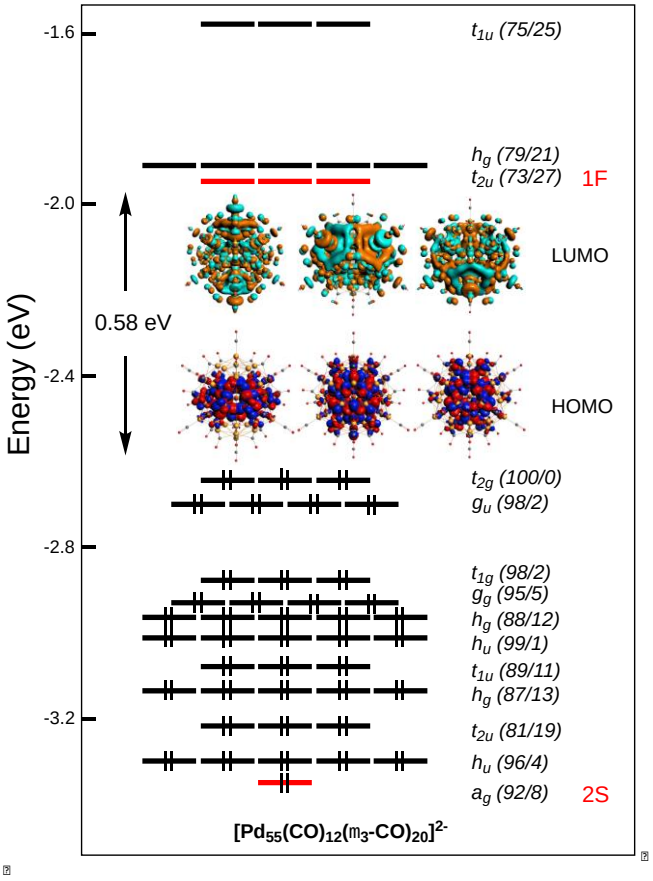

Figure 3. Kohn-Sham molecular orbital (MO) diagram of $[Pd_{55}(CO_{12})(\mu_3\text{-}CO)_{20}]^{2-}$ (I_h symmetry assumed). Values in parenthesis indicate metal/ligand composition (in %). Levels shown in red correspond to *jellium* levels. In I_h symmetry, the vacant 1F level is split into t_{2u} (LUMO) and g_u (lying at higher energy and not shown).

nine of the *5s* combinations. In order to get a deeper understanding on this MO level crossing, we used the opportunity given by the ADF program suite to express the molecular orbitals as linear combinations of the orbitals of two fragments, that we chose to be $[Pd_{55}]^{2-}$ metal kernel and its complete $[(CO)_{32}]$ ligand shell, respectively. Unsurprisingly, single-point spin-restricted calculations (as required by the ADF program) on the $[Pd_{55}]^{2-}$ fragment could not be converged in a reasonable ground state. Excited states were obtained instead. Just to mention, the same situation occurred for the neutral I_h fragment. These results are in line with calculations previously carried out on Pt_{55}.[44] Nevertheless, these results were sufficient for extracting the qualitative bonding picture sketched in Figure 5. For the sake of simplicity the π^*(CO) orbitals are not considered in this diagram, although they play a substantial role in stabilizing the occupied *4d*-block. The unstable $[Pd_{55}]^{2-}$ fragment has 275 (*4d*) + 10 (*5s*) = 285 low-lying combinations, of which 275 + 1 = 276 are occupied.

Assuming formally that nine among the ten *5s* combinations are unoccupied, one is left with the $[Pd_{55}]^{2-}$ MO picture shown on the left of Figure 5. The combinations of the ligand lone pair orbitals interact with the high-lying accepting orbitals on the metal

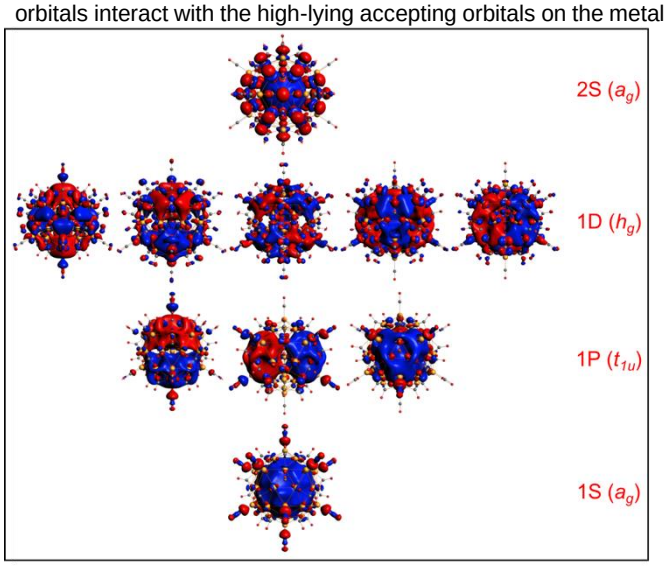

Figure 4. The ten occupied *superatomic* orbitals of $[Pd_{55}(CO_{12})(\mu_3\text{-}CO)_{20}]^{2-}$.

outer shell (*sp*-type), but also with the *4d*-block. This later interaction results in the destabilization of nine *4d* combinations, which in turn transfer their electrons to the mainly unperturbed 1P, 1D and 2S orbitals. This creates a not-very-large but significant HOMO-LUMO gap which provides $[Pd_{55}(CO_{12})(\mu_3\text{-}CO)_{20}]^{2-}$ with a closed-shell configuration for the count of 20 *superatom* electrons. Unfortunately, because of important mixing with π^*(CO) orbitals, it was not possible to individually identify the nine vacant 4*d* combinations. However, a detailed orbital counting allows to determine their symmetry ($a_g + t_{1u} + h_g$), which is the same as that of the nine *superatomic* orbitals to which they transfer their electrons (Figure 5). To conclude this section, it is noteworthy that the two other computed models $[Pd_{55}L_{12}(\mu_3\text{-}CO)_{20}]^{2-}$ (L = PH_3, CNH) provided the same electronic structure as $[Pd_{55}(CO_{12})(\mu_3\text{-}CO)_{20}]^{2-}$.

A peculiarity of these $[Pd_{55}L_{12}(\mu_3\text{-}CO)_{20}]^{2-}$ clusters is that their (unstable) icosahedral Pd_{55} metal kernel needs its ligand outer shell for reaching a closed-shell configuration associated with a "magic" *superatom* electron count. A similar situation was found for another Pd cluster, namely the two-electron *superatomic* cuboctahedral species $[Pd_{13}(\mu_4\text{-}C_7H_7)_6]^{2+}$.[45,46] Our calculations on the $[Pd_{55}L_{12}(\mu_3\text{-}CO)_{20}]^{2-}$ models indicate that this closed-shell configuration is retained when the 12 terminal L ligands are removed, but with a very small HOMO-LUMO gap. Further adding of these 12 ligands results in a substantial

10.1002/chem.202000447

destabilization of the LUMOs, leading to the HOMO-LUMO gaps given in Table 2. We believe that the fact that some metal *d*-type orbitals participate to the bonding with the ligands (i.e., are destabilized and depopulated to the benefit of *superatomic* orbitals) is likely not to be uncommon in Pd or Pt cluster chemistry. Indeed, group-10 metals are at the borderline between middle transition-metal and group-11 elements that tend to keep their *d*-block fully occupied and non-bonding. Indeed, the general MO interacting diagram for

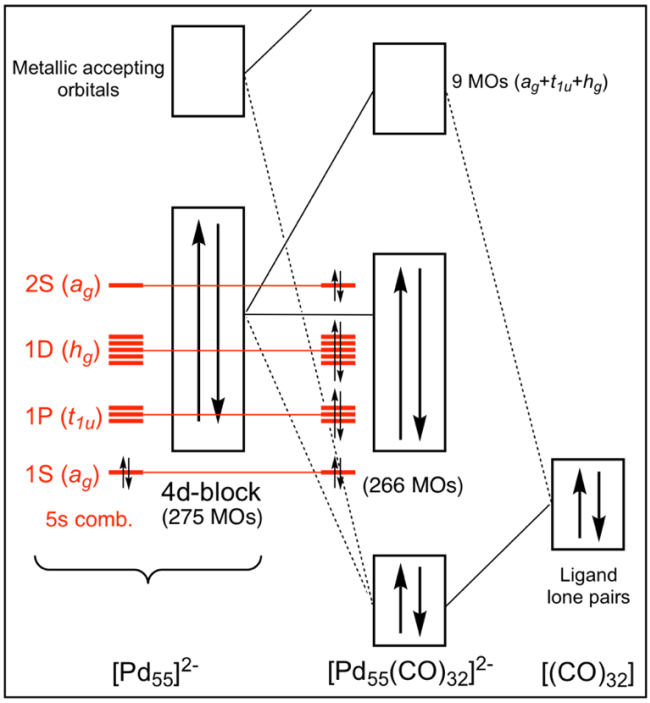

Figure 5. Simplified MO diagram of $[Pd_{55}(CO_{12})(\mu_3\text{-}CO)_{20}]^{2-}$ obtained on the basis of the interaction between the $[Pd_{55}]^{2-}$ and $[(CO)]_{32}$ fragments.

a closed-shell Au, Ag or Cu *superatom* sketched in Figure 6 can be compared to that of Figure 5.

We now return to the discussion on the real charge of Dahl's cluster which is not a dianion, but a neutral species. Removing two electrons from the dianion does not modify the *superatom* electron count since the depopulated orbitals are *4d*-type combinations (Figure 3). As said above, our computed species were found to have triplet ground state configurations. Unfortunately, no explicit mention of the spin state is provided in Dahl's paper for $Pd_{55}(P^iPr_3)_{12}(\mu_3\text{-}CO)_{20}$.[1] No paramagnetic behaviour can be traced from the reported ^{31}P NMR spectrum and unfortunately no NMR ^{1}H or ^{13}C measurements were reported. In any case, regardless of the considered spin state, Jahn-Teller instability is virtually cancelled by the very high cluster compactness of the cluster. Kinetic stability is also expected from the spin density plots of the computed $Pd_{55}L_{12}(\mu_3\text{-}CO)_{20}$ neutral models (Figure 7), which indicate that most of the spin density is confined in the heart of the metallic kernel, with negligible participation of the cluster surface shell (less than 6 %). Thus, low radical reactivity is expected for such species. In fact, another fully characterized example of a 55-atom MacKay *superatom* is known, namely the paramagnetic cluster $[Cu_{43}Al_{12}](Cp^*)_{12}$ (Cp^* = C_5Me_5) with an open-shell 67-electron *superatom* configuration.[47] The kinetic stability of the latter originates from the steric protection of a compact Cp* outer shell. The not yet fully characterized Schmid's cluster (Nanogold®)[48-52] $Au_{55}(PPh_3)_{12}Cl_6$ is also (as well as its monoanion) an open-shell species with the $1S^2\ 1P^6\ 1D^{10}\ 2S^2\ 2P^6\ 1F^{14}\ 1G^9$ *superatomic* configuration.[53]

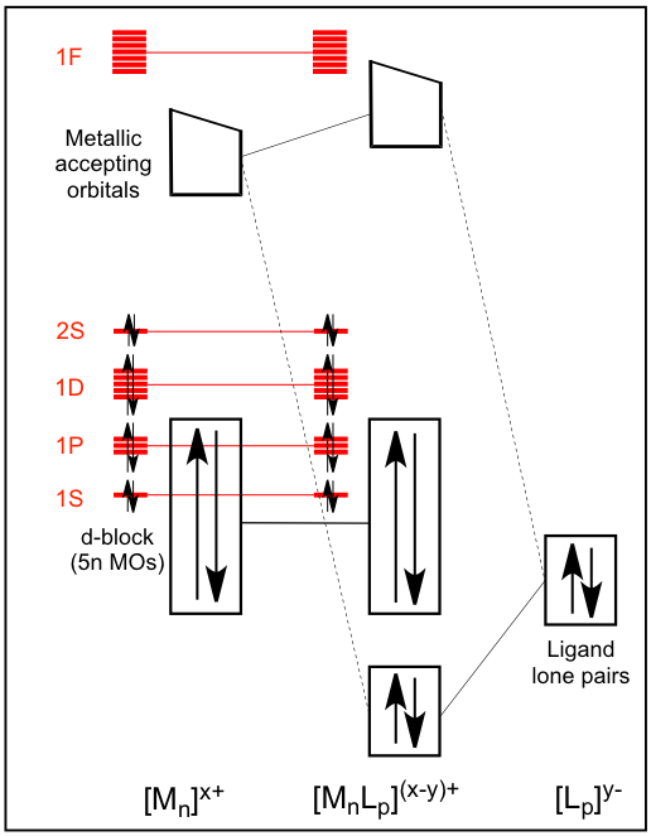

Figure 6. Simplified general MO diagram for a ligated group-11 closed-shell $[M_nL_p]^{(x-y)+}$ *superatom* with an arbitrarily chosen 20-electron "magic" count for a direct comparison with the case of figure 5. Ligands are considered as 2-electron donors, with their formal charges adjusted accordingly (for example, neutral phosphines but anionic thiolates or halogenides).

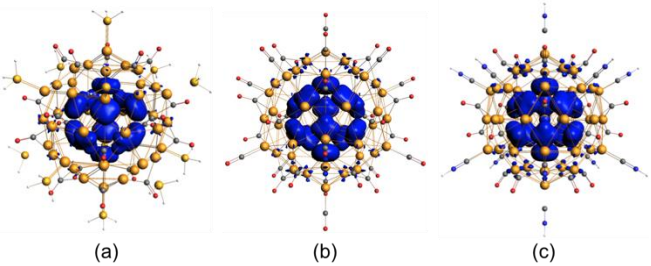

Figure 7. Spin density plots of $Pd_{55}L_{12}(\mu_3\text{-}CO)_{20}$ with L = PH_3 (a), CO (b), CNH (c).

However, its chemical composition and electron count have been debated.[54] Obviously, Mackay compact kernel structures of 55 atoms reaches a size where it starts to behave (somewhat) as a nanoparticle, allowing not a single but a (small) range of electron counts. The upper limit of this range corresponds to the best closed-shell favoured electron count, i.e., the "molecular" favoured count. Such a situation is not so uncommon in transition-metal cluster chemistry. For example, it has been observed in the case of much smaller cobalt-carbonyl clusters.[55,56] The fact that the neutral form of Dahl's cluster was isolated and not its closed-shell dianion is likely to result from the balance of several factors, among which the method of synthesis is one of the most determinant. In any case, $[Pd_{55}L_{12}(\mu_3\text{-}CO)_{20}]$ should be easily be reduced.

Conclusions

We have shown for the first time that the structure of the spherical nanosized cluster $[Pd_{55}L_{12}(\mu_3\text{-}CO)_{20}]$ can be interpreted using the *jellium* model as a regular *superatom*, characterized by the "magic" 20-electron count ($1S^2\ 1P^6\ 1D^{10}\ 2S^2$ configuration). Its open shell nature is associated with 4*d*-type single electrons located deeply on the metal kernel, so that the stability of the cluster is not affected. A favoured closed-shell situation occurs with two additional electrons (dianionic state). This does not modify the *superatomic* 20-electron count. These 20 electrons are located in bonding combinations of 5*s* AOs, which means that, considering the closed-shell dianion, nine 4*d*-type combinations have formally transferred their electrons in nine of the 5*s* MO combinations. This level crossing does not occur on the bare $[Pd_{55}]^{2-}$ kernel. It necessitates the presence of the ligands, which destabilize the nine 4*d*-type MOs and open a HOMO-LUMO gap. This is at variance with group-11 ligated clusters for which no *d*-type to *s*-type electron transfer occurs. The need for the ligand envelope for inducing a closed-shell situation has already been noted in the case of the two-electron *superatom* species $[Pd_{13}(\mu_4\text{-}C_7H_7)_6]^{2+}$.[45,46]

Interestingly, among the flurry of extraordinary diverse nanosized CO/PR_3-ligated icosahedral and ccp/hcp-based (homo/hetero) Pd_n clusters reported over the last 20 years,[28,29] only three conform to the icosahedral Mackay model, namely the title compound, the three-shell 145-metal-atom $Pd_{145}(CO)_x(PEt_3)_{30}$ ($x \approx 60$) cluster compound,[57] and the Pd-Pt four-shell 165-metal-atom $Pd_{164-x}Pt_x(\mu_{12}\text{-}Pt)(CO)_{72}(PPh_3)_{20}$ ($x \approx 7$) cluster compound.[53] It is likely that the *superatom* feature observed for $Pd_{55}L_{12}(\mu_3\text{-}CO)_{20}$ is a general rule that can be applicable to group-10 spherical or nearly spherical ligated clusters such as the Pd_{145} and Pd/Pt_{165} species that contain interior two-shell icosahedral Mackay-type geometries.[57,58] Following this line, we suggest that these palladium spherical clusters are indeed *superatoms* characterized by (at least approximately) "magic" electron counts, these electrons occupying 5*s* (Pd) or 6*s* (Pt) states and resulting from electron transfer from 4*d* (Pd) or 5*d* (Pt) states. We think that such electron transfers are likely to govern the metal-metal bonding in the whole chemistry of these group-10 clusters. Finally, note that the present study is also relevant to catalysis as Pd_{55} clusters are close to the optimal cluster size for maximum catalytic activity of Pd clusters and small nanoparticle catalysts.[59-61]

Acknowledgements

J. W. thanks the China Scholarship Council for a Ph.D. scholarship. The authors are grateful to GENCI (Grand Equipment National de Calcul Intensif) for HPC resources (Project A0050807367). The authors are grateful to the French Research National Agency (ANR-08-BLAN-0079-01) for financial support.

Conflicts of interest

The authors declare no competing financial interest.

Keywords: Palladium nanocluster • Superatom • Mackay icosahedron • Electronic structure •

[1] J.D. Erickson, E. G. Mednikov, S. A. Ivanov, L. F. Dahl, *J. Am. Chem. Soc*. **2016**, 138, 1502-1505.
[2] A. L. Mackay, *Acta Crystallogr*. **1962**, 15, 916.
[3] R. Hoffmann, P. v. R. Schleyer, H. F. Schaefer III, *Angew. Chem. Int. Ed.* **2008**, 47, 7164-7167.
[4] D. M. P. Mingos, D. J. Wales, *Introduction to Cluster Chemistry*, Prentice-Hall, Englewood Cliffs, **1990**.
[5] R. Mason, K. M. Thomas, D. M. P Mingos, *J. Am. Chem. Soc.* **1973**, 95, 3802-3804.
[6] D. M. P. Mingos, R. L. Johnston, *Struct. Bond.* **1987**, 68, 29-87.
[7] D. M. P. Mingos, *Pure. Appl. Chem.* **1991**, 63, 807-812.
[8] J.-Y. Saillard, J.-F. Halet, *Struct. Bond.* **2016**, 169, 157-179.
[9] G. Frapper, J.-F. Halet, A. R. Oganov, A. G. Kvashnin, G. Saleh, in *Computational Materials Discovery (Royal Society of Chemistry)*, London, **2019**, pp. 320–351.
[10] D. M. P. Mingos, *Dalton Trans*. **2015**, 44, 6680-6695.
[11] Z. Lin, T. Slee, D. M. P. Mingos, *J. Chem. Phys.* **1990**, 142, 321-334.
[12] P. Jena, S. N. Khanna, B. K. Rao, *Clusters and Nano-Assemblies: Physical and Biological Systems*, World Scientific, **2005**.
[13] S. N. Khanna, P. Jena, *Phys. Rev. Lett*. **2008**, 51, 13705-13716.
[14] M. Walter, J. Akola, O. L. Acevedo, P. D. Jadzinsky, G. Calero, C. J. Ackerson, R. L. Whetten, H. Grönbeck, H. Häkkinen, *Proc. Natl. Acad. Sci. USA* **2008**, 105, 9157-9162.
[15] H. Häkkinen, *Chem. Soc. Rev.* **2008**, 37**,** 1847-1859.
[16] J. Akola, M. Walter, R. L. Whetten, H. Hakkinen, H. Gronbeck, *J. Am. Chem. Soc.* **2008**, 130, 3756-3757.
[17] H. Hâkkinen, H. in: *Front. Nanosci*. **2015**, 9, (Chap. 8) **T.** Tsukuda, and H. Häkkinen, H. Eds. Elsevier, Oxford, UK.
[18] S. Wang, Q. Li, X. Kang, M. Zhu, *Acc. Chem. Res.* **2018**, 51, 2784-2792.
[19] A. Muñoz-Castro, *Phys. Chem. Chem. Phys.* **2019**, *21*, 13022-13029
[20] E. Roduner, *Phys. Chem. Chem. Phys.* **2018**, 20, 23812-23826.
[21] S. Khanna, P. Jena, *Phys. Rev. Lett.* **1992**, 69, 1664-1667.
[22] J. U. Reveles, S. N. Khanna, P. J. Roach, A. W. Castleman, *Proc. Natl. Acad. Sci.*, 2006, **103**, 18405-18410.
[23] A. W. Castleman, S. N. Khanna, *J. Phys. Chem. C* **2009**, 113, 2664-2675.
[24] S. A. Claridge, A. W. Castleman, S. N. Khanna, C. B. Murray, A. Sen, P. S. Weiss, *ACS Nano* **2009**, 3, 244-255.
[25] W. A. de Heer, *Rev. Mod. Phys.* **1993**, 65, 611-676.

[26] W. D. Knight, K. Clemenger, W. A. de Heer, W. A. Saunders, M. Y. Chou, M. L. Cohen, *Phys. Rev. Lett.* **1984**, 52, 2141-2143.
[27] D. M. P. Mingos, T. Slee, L. Zhenyang, *Chem. Rev.* **1990**, 90, 383-402.
[28] E. G. Mednikov, L. F. Dahl, *J. Chem. Educ.* **2009**, 86, 1135-1135.
[29] E. G. Mednikov, L. F. Dahl, *Philos. Trans. R. Soc. A* **2010**, 368, 1301-1332.
[30] O. Belyakova, Y. Slovokhotov, *Russ. Chem. Bull.* **2003**, 52, 2299-2327.
[31] C. Femoni, M. C. Iapalucci, F. Kaswalder, G. Longoni, S. Zacchini, *Coord. Chem. Rev.* **2006**, 250, 1580-1640.
[32] I. Ciabatti, C. Femoni, M. C. Iapalucci, G. Longoni, S. Zacchini, *J. Clust. Sci.*, **2014**, 25, 115-146.
[33] K.G. Dyall and K. Fægri, Jr., *Introduction to Relativistic Quantum Chemistry*, Oxford University Press, New York, **2007**.
[34] a) G. te Velde, F. M. Bickelhaupt, S. J. A. van Gisbergen, C. F. Guerra, E. J. Baerends, J. G. Snijders, Ziegler, *J. Comput. Chem.* **2001**, 22**,** 931-967; b) ADF2016, SCM, Theoretical Chemistry, Vrije Universiteit: Amsterdam, The Netherlands; http://www.scm.com.
[35] E. van Lenthe, E. J. Baerends, J. G. Snijders, *J. Chem. Phys.* **1994**, 101, 9783.
[36] S.D. Vosko, L. Wilk, M. Nusair, *Can. J. Chem.* **1980**, 58, 1200-1211.
[37] A. D. Becke, *Phys. Rev. A* **1988**, 38**,** 3098-3100.
[38] J. P. Perdew, *Phys. Rev. B* **1986**, 33**,** 8822-8824.
[39] S. Grimme, *J. Comput. Chem.* **2006**, 27**,** 1787-1799.
[40] E. V. Lenthe, E. J. Baerends, *J. Comput. Chem.* **2003**, 24**,** 1142-1156.
[41] E. D. Glendening, J. K. Badenhoop, A. E. Reed, J. E. Carpenter, J. A. Bohmann, C. M. Morales, F. Weinhold, NBO 6.0, Theoretical Chemistry Institute, University of Wisconsin (Madison, WI, **2001**, http://nbo6.chem.wisc.edu).
[42] M. J. Frisch, G. W. Trucks, H. B. Schlegel, G. E. Scuseria, M. A. Robb, J. R. Cheeseman, G. Scalmani, V. Barone, G. A. Petersson, H. Nakatsuji, X. Li, M. Caricato, A. V. Marenich, J. Bloino, B. G. Janesko, R. Gomperts, B. Mennucci, H. P. Hratchian, J. V. Ortiz, A. F. Izmaylov, J. L. Sonnenberg, D. Williams-Young, F. Ding, F. Lipparini, F. Egidi, J. Goings, B. Peng, A. Petrone, T. Henderson, D. Ranasinghe, V. G. Zakrzewski, J. Gao, N. Rega, G. Zheng, W. Liang, M. Hada, M. Ehara, K. Toyota, R. Fukuda, J. Hasegawa, M. Ishida, T. Nakajima, Y. Honda, O. Kitao, H. Nakai, T. Vreven, K. Throssell, J. A. Montgomery, Jr., J. E. Peralta, F. Ogliaro, M. J. Bearpark, J. J. Heyd, E. N. Brothers, K. N. Kudin, V. N. Staroverov, T. A. Keith, R. Kobayashi, J. Normand, K. Raghavachari, A. P. Rendell, J. C. Burant, S. S. Iyengar, J. Tomasi, M. Cossi, J. M. Millam, M. Klene, C. Adamo, R. Cammi, J. W. Ochterski, R. L. Martin, K. Morokuma, O. Farkas, J. B. Foresman, D. J. Fox, (Gaussian, Inc., Wallingford CT, **2016**).
[43] F. Weigend, R. Ahlrichs, *Phys. Chem. Chem. Phys.* **2005**, 7, 3297-3305.
[44] J. L. F. Da Silva, H. G. Kim, M. J. Piotrowski, M. J. Prieto, G. Tremiliosi-Filho, *Phys. Rev. B* **2010**, 82, 205424.
[45] J. Wei, S. Kahlal, J.-F. Halet and J.-Y. Saillard, *J. Clust. Sci.* **2019**, 30, 1227-1233.
[46] M. Teramoto, K. Iwata, H. Yamaura, K. Kurashima, K. Miyazawa, Y. Kurashige, K. Yamamoto, T. Murahashi, *J. Am. Chem. Soc.* **2018**, 140, 12682-12686.
[47] J. Weßing, C. Ganesamoorthy, S. Kahlal, R. Marchal, C. Gemel, O. Cador, A. C. H. Da Silva, J. L. F. Da Silva, J.-Y. Saillard, R. A. Fischer, *Angew. Chem. Int. Ed.* **2018**, 57, 14630-14634.
[48] G. Schmid, R. Pfeil, R. Boese, F. Bandermann, S. Meyer, G. H. M. Calis, J. W. A. van der Velden, *Chem. Ber.* **1987**, 114, 3634-3642.
[49] G. Schmid, *Chem. Soc. Rev*. **2008**, 37, 1909-1930.
[50] G. Schmid, *Chem. Rev.* **1992**, 92, 1709-1727.
[51] G. Schmid, In *Physics and Chemistry of Metal Cluster Compounds*; de Jongh, L. J., Ed.; Kluwer Academic Publ.: Dordrecht/Boston/London, **1994**, Chap. 3, pp 107−134.
[52] G. Schmid, In *Clusters and Colloids: From Theory to Applications*; Schmid, G., Ed.; VCH Publ. Inc.: New York, **1994**, pp 178−211.
[53] A. Muñoz-Castro, personal communication, 2019.
[54] M. Walter, M. Moseler, R. L. Whettende, H. Häkkinen, *Chem. Sci.* **2011**, 2, 1583–1587.
[55] M. Bencharif, O. Cador, H. Cattey, A. Ebner, J.-F. Halet, S. Kahlal, W. Meier, Y. Mugnier, J.-Y. Saillard, P. Schwarz, F. Z. Trodi, J. Wachter, M. Zabel, *Eur. J. Inorg. Chem.* **2008**, 12, 1959-1968.
[56] O. Cador, H. Cattey, J.-F. Halet, W. Meier, Y. Mugnier, J. Wachter, J.-Y. Saillard, B. Zouchoune, M. Zabel, *Inorg. Chem.* **2007**, 46, 501-509.
[57] N. T. Tran, D. R. Powell, L. F. Dahl, *Angew. Chem. Int. Ed.* **2000**, 39, 4121-4125.
[58] E. G. Mednikov, M. C. Jewell, L. F. Dahl, *J. Am. Chem. Soc.* **2007**, 129, 11619-11630.
[59] D. Astruc, *Tetrahedron Asym.* **2010**, 21, 1041-1054.
[60] Y. Du, H. Sheng, D. Astruc, M. Zhu, *Chem. Rev*. **2020**, 120, 526-622.
[61] K. Yamamoto**,** T. Imaoka, M. Tanabe, T. Kambe, *Chem. Rev*. **2020**, 120, 1397-1437.

10.1002/chem.202000447

WILEY-VCH

Entry for the Table of Contents (Please choose one layout)

FULL PAPER

DFT calculations show that the spherical Mackay icosahedral nanosized cluster $Pd_{55}(P^iPr_3)_{12}(\mu_3\text{-}CO)_{20}$ can be considered as a regular 20-electron *superatom*.

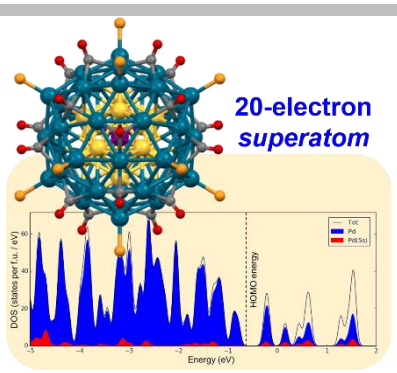

Jianyu Wei, Rémi Marchal, Didier Astruc, Jean-Yves Saillard, Jean-François Halet* and Samia Kahlal**

Page No. – Page No.

Theoretical analysis of the Mackay icosahedral cluster $Pd_{55}(P^iPr_3)_{12}(\mu_3\text{-}CO)_{20}$: An open-shell 20-electron superatom